Atmospheric parameters derived from VGOS sessions observed with the Onsala twin telescopes

Atmospheric parameters derived from VGOS sessions observed with the Onsala twin telescopes

R. Haas, G. Elgered

Abstract We compare the atmospheric parameters derived from the analysis of VGOS sessions that were observed with the Onsala twin telescopes to the corresponding results derived from co-located GNSS stations and a ground-based microwave radiometer at Onsala. The focus is on the first four VGOS Research & Development sessions, observed in 2021 and 2022, aimed at testing scheduling strategies with short scan length in order to obtain a good local sky coverage. The data analysis of all three techniques allows a high temporal resolution of 5 min for the atmospheric parameters. We find high correlation (0.97) for the zenith total delays of the three techniques, and pair-wise weighted root mean square difference on the order of 4–10 mm. The linear horizontal delay gradients are less well correlated (0.4–0.5) and have pair-wise weighted root mean square differences in the sub-mm range.

Keywords VGOS, GNSS, WVR, ZTD, gradients

1 Introduction

The VLBI Global Observing System (VGOS) was designed to achieve one order of magnitude improvement in accuracy and precision for the derived geodetic parameters, compared to the legacy S/X system (Petrachenko et al., 2009). To reach this goal, a number of areas of improvement were identified in the VGOS design phase. One aspect of major concern was turbulence that is affecting the signal delay in the neutral atmosphere (Nilsson and Haas, 2010). One outlined strategy to address this effect is to improve the spatial and temporal sampling of the signal delay introduced by the atmosphere, i.e. more observations per unit of time and in many different local directions. This is implemented by using radio telescopes that move fast in azimuth and elevation, e.g. the Onsala twin telescopes (OTT) (Haas et al., 2019).

During 2021 and 2022 a series of VGOS Research & Development (VR) sessions were scheduled to address the aspect of high spatial and temporal sampling of the local atmosphere. Observatories that are equipped with VGOS stations and co-located instrumentation for other space geodetic and remote sensing techniques, such as Global Navigation Satellite Systems (GNSS) and ground-based microwave radiometers, often called water vapour radiometers (WVR), are perfect sites to assess this new VGOS strategy.

The Onsala Space Observatory (OSO) inaugurated the twin telescopes in 2017. They have been operational in the IVS VGOS observing program since 2019 (Haas et al., 2019). In the following we refer to these two stations as O13E for ONSA13NE and O13W for ONSA13SW. OSO operates also several co-located GNSS stations, including the two stations ONSA and ONS1 that are part of several networks, e.g. the IGS. Additionally, there is a continuously operating WVR at OSO. The VLBI, GNSS, and WVR instruments are co-located within about 600 m distance, thus sharing the local atmosphere at the site. A comparison of the atmospheric parameters derived from the different techniques therefore is a suitable way to assess the accuracy of VGOS when using high spatial and temporal resolution.

Rüdiger Haas · Gunnar Elgered
Chalmers University of Technology, Department of Earth, Space and Environment, Onsala Space Observatory, SE-439 92, Onsala, Sweden

2 Data set

We focus on the first four VR sessions that were observed in 2021 and 2022. These sessions were scheduled using the *VieSched++* software (Schartner and Böhm, 2019) with the aim to generate observing plans with as short as possible scan length in order to achieve as many as possible scans in as many as possible local directions. Doing so, a very dense sampling of the local atmosphere at the participating VGOS stations should be achieved.

Table 1 provides an overview of these first four VR sessions in 2021 and 2022, and the instrumentation operated during these sessions. While both VGOS stations were available for VR2101 and VR2202, unfortunately only one each could participate in VR2022 and VR2203. The two GNSS stations were operating during all four VR sessions, and the WVR was operating during three out of four VR sessions.

Table 1 Overview of the instrumentation operating at OSO during the first four VR sessions in 2021 and 2022.

Session	Date	O13E	O13W	ONSA	ONS1	WVR
VR2101	2021-07-29/30	√	√	√	√	√
VR2201	2022-01-20/21	√	√	√	√	
VR2202	2022-03-17/18	√		√	√	√
VR2203	2022-05-19/20		√	√	√	√

3 Data analysis

We analyzed the VGOS database of the above mentioned four VR sessions with the *ASCOT* software (Artz et al., 2016) using a least-squares analysis and following the analysis strategy used for the IVS ITRF2020 analysis (Gipson, 2020). We applied the VMF3 mapping functions (Landskron and Böhm, 2018) and included data to a minimum elevation cutoff of 5^{o}. The locally observed pressure, from the VLBI logfiles, was the basis for the Zenith Hydrostatic Delays (ZHD). Then Zenith Wet Delay (ZWD) corrections and total linear horizontal gradients (GRAD) were estimated with 5 min temporal resolution using loose constraints. The GRAD parameters were expressed as east (GRE) and north (GRN) components. The a priori ZHD and estimated ZWD were added to calculate the Zenith Total delays (ZTD). The results for O13E and O13W have basically the same formal errors, see Tab. 2.

The data recorded with the co-located GNSS stations ONSA and ONS1 were analysed with the GipsyX software (Bertiger et al., 2020). The analysis used multi-GNSS data, i.e. GPS, Galileo, and GLONASS, with the precise point positioning (PPP) approach (Zumberge et al., 1997). Two daily RINEX-files each were analysed together in order to achieve continuity of the results over day boundaries. A minimum elevation angle cutoff of 7^{o} was used and the VMF3 mapping functions (Landskron and Böhm, 2018) were applied. ZHD were modelled using standard pressure values, while ZWD corrections and total GRAD were estimated with 5 min temporal resolution using loose constraints. As for the VGOS case, the final ZTD were calculated by adding the a priori ZHD and the estimated ZWD. The formal errors of the result derived for both GNSS stations are very similar, see Tab. 2.

The WVR data were observed in a sky-mapping mode and analyzed with an in-house software. An elevation angle cutoff of 25^{o} was used for an unconstrained least-squares analysis (Elgered et al., 2019) with a 5 min temporal resolution. In contrast to VGOS and GNSS is the WVR not sensitive to hydrostatic delays. Thus, the derived atmospheric parameters from the WVR are pure ZWD and pure wet linear horizontal gradients (GRAD-W). In order to be able to compare the WVR results to the results from VGOS and GNSS, ZHD and hydrostatic horizontal gradients (GRAD-H) needed to be added to the WVR results of ZWD and GRAD-W so that the comparisons finally could be done on the basis of ZTD and GRAD. We calculated ZHD based on the locally recorded pressure data at Onsala and added these to the WVR-derived ZWD. For the gradients, we added VMF3-referred horizontal hydrostatic gradients (VMF data server, 2022) that are based on the ERA-Interim numerical weather model data to the WVR-derived gradients. Information on the formal errors for the WVR-derived parameters are provided in Tab. 2

Table 2 Median formal errors of the ZTD (σ_{ZD}) and GRAD (σ_{GE}, σ_{GN}) results derived from VGOS, GNSS, and WVR analysis.

Session	VGOS			GNSS			WVR		
	σ_{ZD}	σ_{GE}	σ_{GN}	σ_{ZD}	σ_{GE}	σ_{GN}	σ_{ZD}	σ_{GE}	σ_{GN}
VR2101	1.61	0.35	0.35	1.42	0.23	0.26	0.37	0.15	0.16
VR2201	1.13	0.24	0.23	1.44	0.24	0.28	–	–	–
VR2202	1.15	0.23	0.25	1.43	0.23	0.25	0.20	0.09	0.10
VR2203	1.08	0.22	0.24	1.42	0.26	0.27	0.30	0.13	0.15

To do a meaningful comparison of the ZTD from VGOS, GNSS and WVR, their values need to be referred to the same reference height. We chose the common reference height to be the GNSS reference point of the station ONSA. Thus, we applied corresponding height corrections (Rothacher et al., 2011), since the reference points of the different instruments are at different heights. However, for the GRAD parameters, no further corrections were needed.

4 Comparisons of atmospheric parameters

OSO operated its VGOS twin telescopes, several GNSS stations, and a WVR, during the four VR sessions. However, only during VR2101 all five instruments were operated, while for the other VR sessions only four out of five could not be operated, see Tab. 1. Nevertheless, we had the possibility to compare all three techniques, VGOS, GNSS and WVR, for three out of the four VR sessions.

In the following, we present several steps of comparisons. We start with the VGOS-internal comparison using VR2101 and VR2201. Then we present the GNSS-internal comparison using all four VR sessions. Finally, we perform the three-technique comparisons with the VR sessions where all three techniques were operated. Here we focus on one station each for VGOS and GNSS, respectively, to be representative for the corresponding technique and to be compared to the WVR results.

4.1 VGOS-internal comparisons

Both VGOS stations, O13E and O13W, participated in VR2201 and VR2202. The derived ZTD and GRAD results agree well. Statistical information in terms of correlation coefficient ρ, offset δ, and standard deviation σ, after subtracting the offset, is provided in Tab. 3. The correlation coefficients are 0.99 for the ZTD, and at least for VR2101 also above 0.93 for the gradients. The low GRAD correlation for VR2201 is simply because there were no significant variations in the gradients during the session. The offsets and standard deviations are all less than or on the order of the formal errors.

Table 3 Statistical information on the agreement of the results derived from VGOS stations O13E and O13W in terms of correlation coefficient ρ, offset δ (O13E-O13W), and standard deviation σ after subtracting the offset.

Session	ZTD			GRE			GRN		
	ρ	δ mm	σ mm	ρ	δ mm	σ mm	ρ	δ mm	σ mm
VR2101	0.99	-0.59	0.73	0.93	-0.05	0.20	0.94	-0.05	0.17
VR2201	0.99	-0.51	0.98	0.54	0.02	0.24	0.53	-0.07	0.34

4.2 GNSS-internal comparisons

The GNSS stations ONSA and ONS1 were operated during all four VR sessions. As for VGOS, the level of agreement between the results derived from the two stations is as expected very high. Statistical information in terms of correlation coefficient ρ, offset δ (ONSA-ONS1), and standard deviation σ after subtracting the offset, is provided in Tab. 4. The correlation coefficients for ZTD are all 0.98 or higher. The ZTD offsets on the order of 2–3 mm are detected, which might indicate that the correction for the height difference between the stations needs to be revisited. The remaining standard deviations after removing the offsets are slightly larger than the formal errors. The correlation coefficients of the GRAD parameters are not as high and vary between the VR sessions. Values of up to 0.79 are seen, and the lowest ones relate to VR2201, the same VR session where the GRAD parameters had low correlation coefficients. Offsets for GRAD parameters are insignificant, and the remaining standard deviation after removing the offsets are about twice as large as the formal errors.

Table 4 Statistical information on the agreement of the results derived from GNSS stations ONSA and ONS1 in terms of correlation coefficient ρ, offset δ (ONSA-ONS1), and standard deviation σ after subtracting the offset.

Session	ZTD			GRE			GRN		
	ρ	δ mm	σ mm	ρ	δ mm	σ mm	ρ	δ mm	σ mm
VR2101	0.99	-1.92	1.78	0.79	0.03	0.47	0.70	0.01	0.42
VR2201	0.99	-2.94	2.06	0.26	-0.12	0.44	0.39	0.04	0.44
VR2202	0.98	-3.42	1.83	0.56	-0.04	0.41	0.75	0.04	0.46
VR2203	0.99	-2.64	1.81	0.67	-0.01	0.44	0.65	0.01	0.49

4.3 VGOS-GNSS-WVR comparisons

For three out of the four VR sessions all three techniques, i.e. VGOS, GNSS, and WVR, could be compared. The ZTD times series are presented in Fig. 1. These graphs show that the VGOS and GNSS results for ZTD follow each other very nicely, including small features variations. It also is visible that the WVR for some periods deviated a bit, e.g. in the second half of VR2101 (top plot) and around 21:00–00:00 during VR2203 (bottom plot), possibly due to high amounts of liquid water and/or less accurate calibrations. It appears that session VR2202 provided the most reliable results from the WVR. As an example, we therefore present the GRAD time series of VR2202 in Fig. 2. The GRAD parameters agree well and also here the small features are picked up by all three techniques.

Table 5 summarizes the average statistical agreement between the three techniques. This is expressed as average values for correlation coefficient (ρ) and the weighted root mean square (wrms) deviation. The average for the correlation coefficients for ZTD is 0.97 for all three pairwise comparisons. The average correlation coefficients for the gradient parameters are about 0.4 but do not reach 0.5 for any of the three pairwise comparisons. The highest value is seen for the north gradient for the comparison of VGOS and GNSS. Both space geodetic techniques reach just 0.42 and 0.44 as correlation coefficient for GRN and GRE when comparing to WVR. We see that the average ZTD wrms for the space geodetic techniques is of the order of 4 mm, while the ZTD wrms difference between the space geodetic techniques and the WVR are of the order of 10 mm. Also for the gradients we see lower wrms values for the comparison of the space geodetic techniques than when comparing the space geodetic techniques with the WVR. However, in all comparison cases, the wrms for the GRAD parameters are sub-mm.

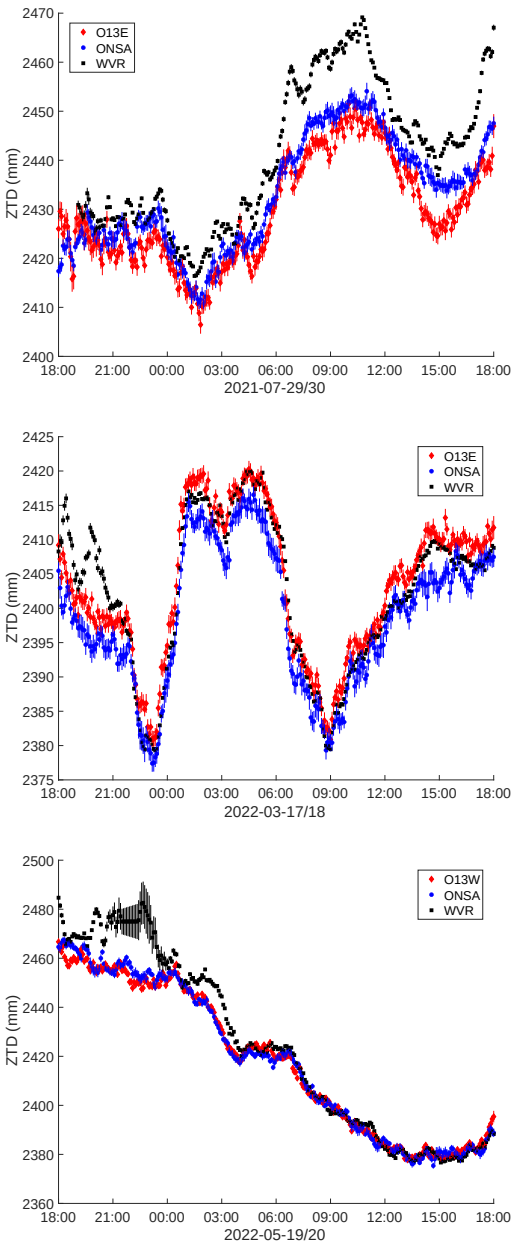

Fig. 1 Time series of ZTD derived from VGOS (red), GNSS (blue) and WVR (black) for VR2101 (top graph), VR2202 (middle graph) and VR2203 (bottom graph).

5 Conclusions and outlook

We compared atmospheric parameters in terms of ZTD and GRAD results for four VR sessions observed in 2021 and 2022. The focus was on simultaneous observations with the co-located instrumentation at Onsala, including two VGOS stations, two GNSS stations, and a WVR. Results for ZTD and GRAD could be determined from independent analyses with an identical temporal resolution of 5 min. To achieve such a high sampling with VGOS was possible thanks to the special scheduling of the VR sessions, aiming as short scan length and high number of well distributed observations. The comparison of the results reveals that the ZTD of all three tech-

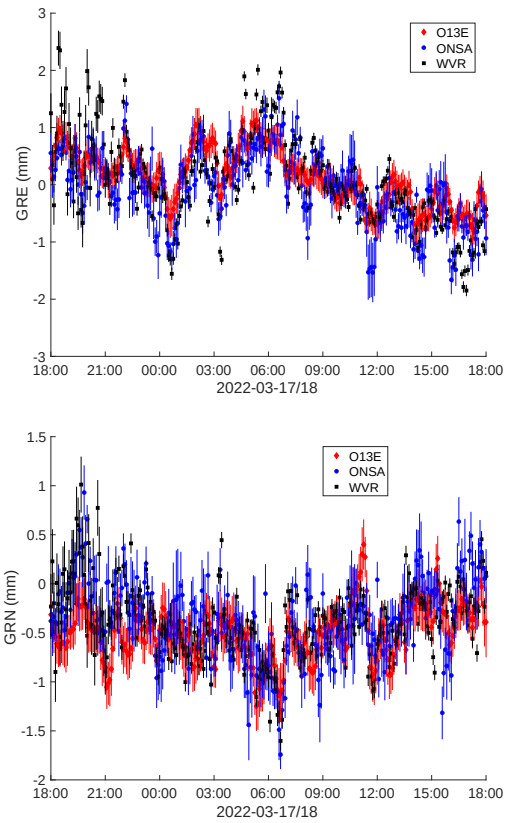

Fig. 2 Time series of gradients GRE (top) and GRN (bottom) derived from VGOS (red), GNSS (blue) and WVR (black) for VR2202.

Table 5 Statistical information on the agreement of the results derived from VGOS, GNSS and WVR. Listed are average values for correlation coefficient (ρ), and average weighted root-mean square (wrms) deviation.

	ρ	WRMS (mm)	ρ	WRMS (mm)
ZTD	GNSS		WVR	
VGOS	0.97	4.04	0.97	10.47
GNSS	–	–	0.97	9.89
GRE	GNSS		WVR	
VGOS	0.44	0.58	0.44	0.87
GNSS	–	–	0.44	0.95
GRN	GNSS		WVR	
VGOS	0.47	0.50	0.42	0.87
GNSS	–	–	0.42	0.87

niques show very high correlation, but still suffer from so-far unexplained offsets on the order of 5–10 mm. The results for gradient parameters are less well correlated and have offsets in the sub-millimetre range. As expected the two space geodetic techniques agree in general slightly better than each one of them agrees with the WVR.

We focused on only four VGOS sessions and thus suffer from a low number of data points. A larger data set is needed in order to draw further conclusions. Thus, we plan to perform similar analyses with as many as possible VGOS sessions observed at Onsala. Also different analysis approaches need to be tested, e.g. different temporal resolutions and constraints.

References

Artz T et al. (2016) ivg::ascot: Development of a new vlbi software package. In: Behrend, Baver, Armstrong (eds) *IVS 2016 General Meeting Proceedings*, **NASA/CP-2016-219016**, 217–221, https://ivscc.gsfc.nasa.gov/publications/gm2016/045_artz_etal.pdf

Bertiger W et al. (2002) GipsyX/RTGx, a new tool set for space geodetic operations and research. *ASR*, 66(3), 469–489, doi:10.1016/j.asr.2020.04.015

Elgered G et al. (2019) On the information content in linear horizontal delay gradients estimated from space geodesy observations, *AMT*, 12, 3805–3823, doi:10.5194/amt-12-3805-2019

Gipson J (2020) IVS Checklist for ITRF2020. https://ivscc.gsfc.nasa.gov/IVS_AC/ITRF2020/ITRF2020_checklist_v2020Jan13.pdf

Haas R et al. (2019) Status of the Onsala twin telescopes – two years after the inauguration. In: Haas, Garcia-Espada, Lopez Fernandez (eds) *Proc. 24th EVGA working meeting*, ISBN: 978-84-416-5634-5, 5–9.

Landskron D, Böhm J (2018) VMF3/GPT3: refined discrete and empirical troposphere mapping functions. *J Geod*, 92, 349–360, doi:10.1007/s00190-017-1066-2

Nilsson T, Haas R (2010) Impact of atmospheric turbulence on geodetic very long baseline interferometry. *JGR* 115(B3), doi:10.1029/2009JB006579

Ning T, Elgered G (2021) High-temporal-resolution wet delay gradients estimated from multi-GNSS and microwave radiometer observations. *AMT*, 14, 5593–5605, doi:10.5194/amt-14-5593-2021

Petrachenko B et al. (2009) Design aspects of the VLBI2010 system. **NASA/TM-2009-214180**

Rothacher M et al. (2011) GGOS-D: homogeneous reprocessing and rigorous combination of space geodetic observations. *J Geod*, 85(10):679–705, doi:10.1007/s0019 0-011-0475-x

Schartner M, Böhm J (2019) VieSched++: A New VLBI Scheduling Software for Geodesy and Astrometry. *PASP*, 131:084501, doi:10.1088/1538-3873/ab1820

re3data.org: VMF Data Server; editing status 2020-12-14; re3data.org - Registry of Research Data Repositories, doi:10.17616/R3RD2H

Zumberge J F et al. (1997) Precise Point Positioning for the efficient and robust analysis of GPS data from large networks. *JGR*, 102(B3), 5005–5017, doi:10.1029/96JB03860